Danish Meteorological Institute
Ministry for Climate and Energy

Danish Climate Centre Report 08-07

QUANTIFY: Modelling air-plane contrails with the IFSHAM general circulation model

Marianne Sloth Madsen and Peter Thejll

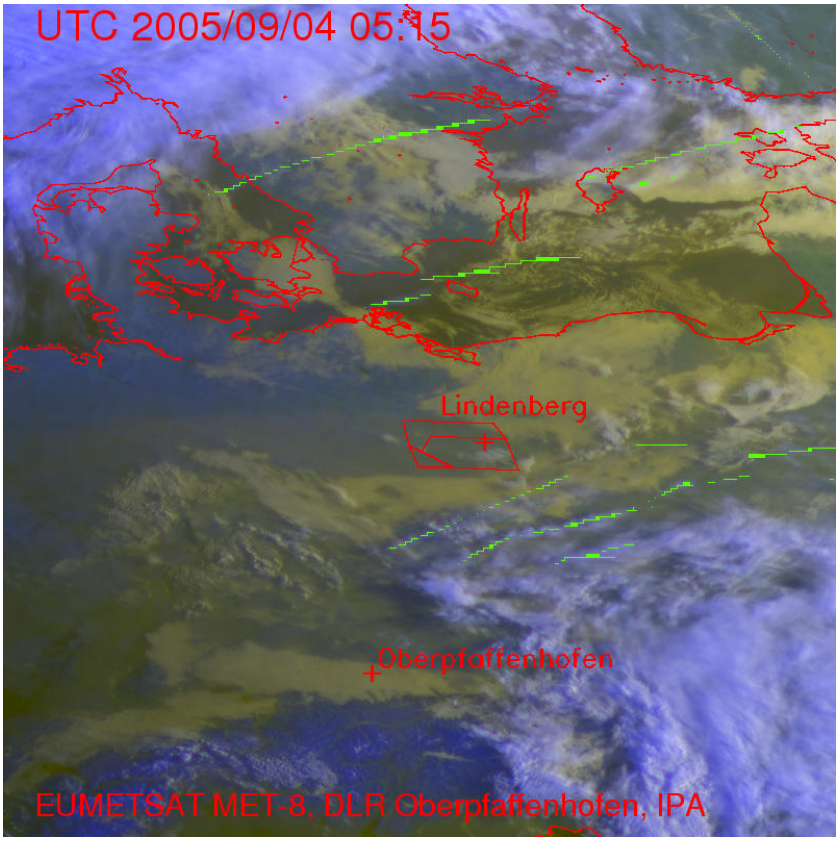

Colophone

Serial title:
Danish Climate Centre Report 08-07

Title:
QUANTIFY: Modelling air-plane contrails with the IFSHAM general circulation model

Subtitle:
Authors:
Marianne Sloth Madsen and Peter Thejll

Other Contributers:
Responsible Institution:
Danish Meteorological Institute

Language:
English

Keywords:
QUANTIFY, air-plane contrails, cloud formation

Url:
www.dmi.dk/dmi/dkc08-07

ISSN:
1399-1957

ISBN:
978-87-7478-566-8 (online)

Version:
1

Website:
www.dmi.dk

Contents

1. Dansk resumé

Dette projekt er en del af EU-projektet QUANTIFY som sigter mod at undersøge hvordan transport påvirker klimaet. Formålet med denne del af projektet er at undersøge hvordan kondensstriber fra højtflyvende fly spredes af vindene i den øvre troposfære. Der er blevet udviklet et sæt af subrutiner, der beskriver dannelse og spredning af specifikke kondensstriber baseret på virkelige flytrafikdata. Dette modul er koblet til IFSHAM modellen og vi har brugt den såkaldte nudging-teknik for at få modellen til at følge de aktuelle atmosfæriske betingelser så godt som muligt. Vi har brugt data for flytrafikken over Tyskland i september 2005.

Ideelt set kan satellitbilleder af contrails bruges til at validere modellen og tune de parametre, der bruges til at definere dannelseskriterier og spredningshastighed. Vi har kørt modellen for et stort antal forskellige parameter-kombinationer. og undersøgt, hvordan vi kan evaluere eksperimenterne ved at sammenligne med sattellitbillederne.

I praksis er det en vanskelig opgave, og det har ikke været muligt at parre enkelte modellerede kondensstriber med observerede striber. Den algoritme der bruges til at detektere kondensstriber i sattellitbillederne kan kun detektere nye, lineære kondensstriber og dermed kun en lille fraktion af de kondensstriber modellen danner. Samtidig sker der ofte fejldetektioner af skykanter, floder etc. Modellens resultater er mere entydige, men resolutionen er forholdsvis grov (110x110km) og der er en vis usikkerhed på de meteorologiske felter.

Sammenligningen må altså baseres på regionale og tidsmæssige variationer i fordelingen af kondensstriber. Vi har brugt en stokastisk metode og en simplere point-metode til at beskrive hvor god en sammenlignelighed der er mellem model og billede for de forskellige sæt af parametre. De to metoder giver forskelligt resultat, men indikerer begge at tærskelværdien for relativ fugtighed skal være større end 0.7. Sammenligneligheden øges markant, når der tages højde for den optiske dybde, og kun modellerede kondensstriber, der ville kunne detekteres tælles med.

2. Abstract

This work is part of the QUANTIFY project and aims at quantifying the effects of airplane contrails. We have implemented a contrail module which describes the formation, evolution and transport of contrails in the IFSHAM general circulation model. The model is based on real air traffic data for Germany during September 2005 and is forced towards the observed atmospheric state by using the nudging technique . We have investigated how satellite images can be used to tune model parameters. The comparison is not straight forward due to model limitations and problems concerning the detection algorithm used to encode the satellite images. First, we have done visual inspection image by image to investigate the match between observed and modelled contrails. We have not been able to match any contrails track-by-track, rather we need to consider the regional and diurnal distribution. Second we have run the model for a large number of combinations of model parameters. These include the parameters entering the formation and persistence criteria and those determining the evolution.
We evaluated the experiments using a stochastic scoring method and a simpler odds ratio. The two methods do not agree on the best choice of model parameters.
Counting only visible contrails with an optical depth larger than a certain threshold gave a significantly better match between regions where contrails occur and not.

3. Introduction

The QUANTIFY project is an EU FP6 project that generally seeks to quantify the impacts of various modes of transportation systems on climate. We are engaged in a part of that project, relating to quantifying and studying the impacts of air-plane contrails. In particular, we are engaged in modelling the formation, evolution and transport of contrails by tuning particular algorithms by comparison to satellite images of Europe. The project work was originally started by Annette Guldberg who set up the main parts of the contrail module in collaboration with Klaus Gierens.

Contrail modelling has previously been performed at DMI as described in Ref. [Guldberg and Nielsen, 2004]. In the previous work the radiative forcing due to contrail formation was estimated using the IFSHAM general circulation model extended with the Ponater et al. [Ponater et al., 2002] contrail parameterisation. This parameterisation is linked to the Sundqvist [Sundqvist, 1978] cloud scheme and basically calculates the potential contrail cover. The actual contrail cover was then obtained by tuning the model to match the total observed global contrail cover.

The study described here does not consider the forcing impact, rather the aim is to consider specific contrails and model their evolution and spreading into cirrus clouds. Since the study is based on real aircraft data it is possible to investigate how well the modelled contrails match with those observed by satellites.

The report describes the contrail module that has been developed and implemented in IFSHAM to study the evolution of specific contrails. It also includes analysis of results from a large number of model runs with different sets of parameters. These parameters are used to describe the criteria for contrail persistence and the time-development of the contrail spreading and ideally we should be able to tune these parameters by comparison with the satellite images. The tuned model will be of use in future modelling of contrails where their impact on climate is further evaluated.

This report is structured as follows. In Chapter 4 we describe how the GCM code was modified to include contrail-specific modules relating to formation criteria and to contrail transport, evolution and termination. In section 4.2 we describe the *nudging* required during the model runs in order to force the solution close to real conditions. In section 5 we investigate how satellite images can be used to tune the parameters used in the contrail model. The investigation is based on a combination of different statistical methods and direct comparison looking for a one-to-one match between model and observation.

4. Contrail modelling

The contrail module has been implemented in the IFSHAM general circulation model. The IFSHAM model has been developed at DMI by Shuting Yang [Yang, 2004] as a combination of the dynamical core from ARPEGE/IFS [Déqué et al., 1994] and the physical parameterisation package of ECHAM5 [Roeckner et al., 2003]. The model is a spectral primitive equation model and uses a linear reduced Gaussian grid. For this study, the IFSHAM model has been run with spectral truncation Tl159 using 160 latitude and 320 longitude points and a vertical resolution of 31 layers. Climatological sea surface temperatures are adopted.

The IFSHAM code has been extended by a contrail module that is called at the end of each time step. The contrail module consists of a set of subroutines that handle the read-in of air-plane positions and the subsequent formation of contrails. Next, persistent contrails are advected, spread by the wind shear and finally terminated when the criteria for contrail persistence are no longer fulfilled. The contrail module uses a number of fields from the climate model whereas contrail information is not passed back to the model but written out for analysis.
A flow-chart of the contrail subroutines is shown in Figure 4.1.

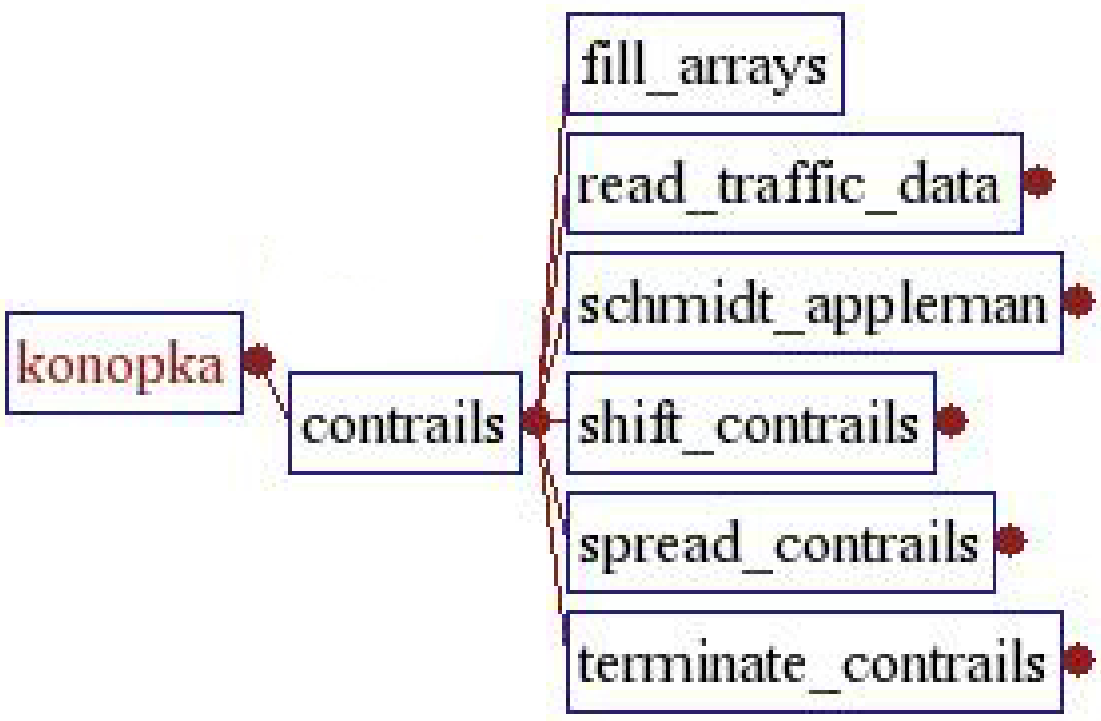

Figure 4.1: Schematic flow-chart of the contrails module.

4.1 Formation and evolution of contrails

At the beginning of each call to the contrail module, air traffic data is read in. Our input data file is based on actual air traffic data as obtained during the PAZI campaign (Personal communication, K. Gierens). It contains flight information given as longitudes, latitudes, headings, flight numbers and times. We have files covering Germany for the whole month of September with a time resolution of 1 second. Since we use a model time step of 1800 seconds, all points corresponding to the last 1800

seconds are read in during each call to the contrail module but reference is still kept to the actual age of the point as obtained from the flight traffic file. We only use positions above 376 mb as this corresponds to the regions where contrails are expected to form.
In the next subroutine we investigate whether the Schmidt-Applemann criterion [Schumann, 1996] is fulfilled so that contrails are formed. For contrails to form the air must be cold and humid. The threshold temperature used in the Schmidt-Applemann condition is given by [Schumann, 1996]

$$T_{contr} = -46.46 + 9.43\ln(G - 0.053) + 0.72(\ln(G - 0.053))^2 \tag{4.1}$$

where

$$G = \frac{EI_{H_2O} c_p p}{\epsilon Q(1-\eta)} \tag{4.2}$$

Here, EI_{H_2O} is the emission index of water, c_p the specific heat at constant pressure, p the pressure, ϵ the ratio of the molecular masses of water and air, η the propulsion efficiency of the jet engine and Q the specific combustion heat. Contrails are only allowed to form if the environmental temperature is lower than T_{contr}. The second criterion is that the ambient relative humidity must exceed the critical relative humidity given by

$$r_{contr(T)} = \frac{G \cdot (T - T_{contr}) + e^L_{sat}(T_{(contr)})}{e^L_{sat}(T)} \tag{4.3}$$

where e^L_{sat} is the saturation pressure of water vapour with respect to the liquid phase. The Schmidt-Applemann condition was implemented in IFSHAM by Annette Guldberg [Guldberg and Nielsen, 2004] and Klaus Gierens.
Furthermore, an environment super-saturated with respect to ice is required for contrail persistence and since contrails are generally not observed during strong subsidence [Duda et al., 2004], a constraint is also set on the vertical wind velocity. The model conditions for contrail persistence are thus

$$RHi > RHi_{persist} \tag{4.4}$$
$$V_{vertical} > V_{vertical,crit} \tag{4.5}$$
$$\tag{4.6}$$

where RHi is the relative humidity in the grid-box holding the contrail. $RHi_{persist}$ and $V_{vertical,crit}$ are local parameters. For all flight tracks these conditions are used to test whether a contrail is formed or not. To apply the condition we need the model temperature, humidity and wind field and a number of parameters have to be set. The values of $RHi_{persist}$ and $V_{vertical,crit}$ are of course important for the number of predicted contrails and we will consider how to tune these parameters in section 5.

For every time-step, persistent contrails are advected horizontally and vertically by the wind field in the given grid-box. Newly formed contrails are only advected according to their respective lifetimes. The contrails spread by atmospheric turbulence and shear and thereby develop into cirrus clouds. In

the model, this is described by a Gaussian plume model [Konopka, 1995, Schumann et al., 1995] which predicts the contrail width as a function of age using the vertical wind shear and a constant diffusivity tensor. At the end of each call to the contrail module, it is tested whether the conditions for super-saturation and vertical wind velocity are still satisfied after advection and spreading, otherwise the given contrail is terminated. For all surviving contrail points, information of location, age, width and original flight number are stored and used as input in the next time step together with a number of new flight tracks. A width criterion has also been included in the termination routine so that very old contrails automatically terminate. We have used a threshold width of 30 km and only a few contrails survive to this width.

4.2 Nudging

The above algorithm could be carried out with atmospheric data from e.g. a reanalysis because the contrails themselves do not impact the structure of the atmosphere. However, reanalysis is not available with high time resolution so the GCM is used to provide model fields at a high cadence (every half hour). A model cannot be started from a given state and then be expected to evolve like reality, even if the original starting condition was very precise - therefore we must 'nudge' the model [Jeuken et al., 1996, Guldberg et al., 2005] towards a realistic state at regular intervals.

The model prognostic variables are thus relaxed towards a reference data set at each model time step.

$$\Phi(t+\Delta t) = \Phi^*(t+\Delta t) + \Delta t \frac{\Phi^{REF}(t+\Delta t) - \Phi^*(t+\Delta t)}{\tau} \tag{4.7}$$

Here the index $*$ indicates the preliminary value of the prognostic variable before nudging and REF denotes the reference value. Δt is the time-step length and τ is the relaxation time. We have used a two-level semi-implicit time stepping scheme and a time-step of 30 minutes. The variables assimilated are temperature, vorticity, divergence, logarithm of surface pressure and surface temperature. We have used ECMWF reanalysis as the reference data set. Six hourly global restart files for September 2005 were provided by Michel Déqué in Tl159L60R resolution and converted to our resolution with 31 vertical layers. The relaxation is done at every time step and a cubic spline interpolation is used to obtain reference data at intermediate times.

The relaxation times have to be specified before the model run. To find the best set of parameters we did a number of runs using different combinations of relaxation times for the five assimilated variables. The best combination was chosen as the one giving the best results for winds in the upper troposphere. We base our parameter search on perturbations of a basic set of parameters given by the `namelist` entry in Figure 4.2. The given values correspond to $G = \frac{\Delta t}{\tau}$.

We evaluate the nudging experiments by calculating the root mean square error on the u-component of the wind in the layers between 100 and 300 hPa on September 6 2005 at longitudes 4 to 52 degrees E and latitudes 48 and 49 degrees N, by comparison to the NCEP reanalysis daily-mean winds. We cannot compare to ERA40 or the JRA25 as they do not, yet, cover the year 2005. Linear interpolation in space and time is performed with the IDL function INTERPOLATE applied to the spatial part and additional weighting on the winds for the day before and after the target point in time - this is needed because INTERPOLATE in IDL only handles up to and including 3-dimensional arrays. The model run was started at midnight between September 4 and 5 and run for 2 days with

```
&NAMNUD
LNUDG=.TRUE.
NFNUDG=7,
NTNUDG=1,
XNUDTE=0.04167,
XNUDDI=0.02083,
XNUDVO=0.16667,
XNUDLP=0.04167,
XNUDST=0.02083,
/
```

Figure 4.2: Basic set of G parameters.

Table 4.1: Nudging experiments. RMSE based on upper tropospheric winds for a given date and region, compared to NCEP winds. See text for further explanations. The asterisk indicates the best nudging experiment. The model time step is 30 minutes unless another value is stated.

Experiment name	Difference from Basic Set	RMSE
Basic set- see Fig. 4.2		4.2177
B 'hard' nudging	all=1	4.4478
C no nudging	all=0	5.2875
time-step	all=0 but 15 min time-step	7.0281
D milder divergence nudging	XNUDDI=0.01042	4.2385
F divergence nudged harder	XNUDDI=0.04167	4.2007
N even harder divergence nudging	XNUDTE=0.01042,XNUDDI=0.06000,XNUDVO=0.08333,	4.0926
G harder T nudging	XNUDTE=0.08335	4.2902
H mild T nudging	XNUDTE=0.02083	4.1958
L even milder T nudge.	XNUDTE=0.01042	4.1943
O T yet even milder nudged	like N, but XNUDDI=0.04167,XNUDTE=0.007,	4.0808
E humidity nudged	XNUDSH=0.02083	4.2333
J Harder vorticity nudging	XNUDVO=0.33334	4.4138
K milder vorticity nudging	XNUDVO=0.08335	4.1012
P Vorticity even milder nudged	XNUDTE=0.007,XNUDDI=0.04167,XNUDVO=0.04333	*4.0650
M a combination of some good values	XNUDVO=0.08335,XNUDTE=0.01042,XNUDDI=0.04167	4.0830

nudging every 1800 seconds, using ECMWF analysis data. The experiments we performed and the results are summarised in Table 4.1.

Generally, the error between NCEP and model is large (4 to 5 m/s, which is 20 or 30% of the mean wind at that altitude), and we speculate that this is due to use of NCEP reanalysis data instead of ECMWF analysis data. The model is nudged by ECMWF analysis values and the two datasets are not expected to be identical. We see that the largest error occurs when no nudging is performed. The difference grows with time - we are looking at day two and if we let more time pass a larger difference would be seen. By using nudging we can reduce the error by 23%, so far - it is possible to improve slightly more by searching the nudging parameter space. It would seem that the original set of nudging parameters (see Figure 4.2) is hard to improve a lot on. We note that the much worse result obtained with a halved time step is not to be interpreted as if this time step inherently is a bad choice - the model probably needs to be re-calibrated given a new time step, and we did not pursue that avenue further. The G values given in Figure 4.3 are used for the model runs discussed in this report unless otherwise stated. These correspond to relaxation times of 48 hours for temperature, 12 hours for divergence, 6 hours for vorticity, 12 hours for the logarithm of surface pressure and 24

hours for surface temperature.

```
 &NAMNUD
LNUDG=.TRUE.
NFNUDG=7,
NTNUDG=1,
XNUDTE=0.01042,
XNUDDI=0.04167,
XNUDVO=0.08333,
XNUDLP=0.04167,
XNUDST=0.02083,
 /
```

Figure 4.3: Optimised set of G parameters used for the IFSHAM model at DMI. Close correspondence to NCEP stratospheric winds was sought.

```
 &NAMNUD
 LNUDG=.TRUE.
 NFNUDG=7,
 NTNUDG=1,
 XNUDTE=0.02083,
 XNUDSH=.00000,
 XNUDDI=0.01042,
 XNUDVO=0.08333,
 XNUDSV=0.,
 XNUDLP=0.02083,
 XNUDST=0.02083,
 XNUDSM=0.,
 XNUDRM=0.,
 XNUDSD=0.,
 /
```

Figure 4.4: Additional set of G parameters used for just one model run (AE2 - see Table 6.4).

5. Calibration of the model

Basically, we have got two sets of parameters. The first set determines the criteria for contrail formation and persistence and includes threshold values for relative humidity $RHi_{persist}$ and vertical velocity $w_{persist}$. It also includes the parameter η which describes the efficiency of the jet engine and enters the formation condition. The second set of parameters refer to the Gaussian plume model used to evaluate the time-dependent spreading of persistent contrails. The important parameters include horizontal and vertical diffusion constants (D_h, D_v), the initial contrail width along with additional tuning parameters.

5.1 Methods

At an early stage we realized that model contrails could not be compared on a one to one basis with observed contrails. First of all, not all real contrails are detected by the image analysis routine used (Mannstein, et al, 1999), and second, the model contrails are in a range of widths - some of which simply would never be detected in real images, and third, model contrails can only be expected to appear roughly where the real contrail is due to a range of issues having to do with model limitations such as length of time steps, horizontal resolution of the model, etc. These problems preclude a pixel-to-pixel comparison of observed contrails and modelled ones. >From [Mannstein, et al. 1999] we gather that the contrail detection routine is sensitive to contrails with widths up to 4 km, and therefore restricted our analysis to model contrails narrower than 4 km.

As we receive a model-map of contrails each half hour (determined by the 1800s time-step of the GCM) we compare these to satellite images taken at the same moment and construct a metric that numerically relates how well the model did. The metric is accumulated for images over a certain period and a final mean score reported. This same score is then calculated for all model runs and thereby a 'best' model can be found.

We also employ the 'odds ratio' method of Stephenson (2000), as used in Tompkins et al (2007) in order to compare two methods.

Our information from satellites is in the form of JPG files each 15 minutes for one month in a region over Germany. In these colour images contrails detected by the Mannstein algorithm had been marked with greenish-blue pixels. We extracted image coordinates for these contrails by selecting pixels on the basis of their G and B pixel values (ignoring the R value). Our criterion was G $>$ 140 and B $<$ 10. Pixel coordinates were then converted to geographic coordinates using a mapping function provided by Herman Mannstein (private communication, 2008).

5.1.1 Visual inspection of contrail numbers

As a simple test of model performance we counted the number of pixels detected as contrails in the satellite images and in scenes generated for the same times from models. While the numbers will not have the same magnitude due to differences in definition of an observed contrail pixel and a point from the model routine, their time-series should correlate well if the model is accurate. In Figure 5.1 we see the number of observed contrails do not go towards zero near each midnight, while the models do. We also see that some day-long episodes of 'many observed pixels' are not well matched by the model.

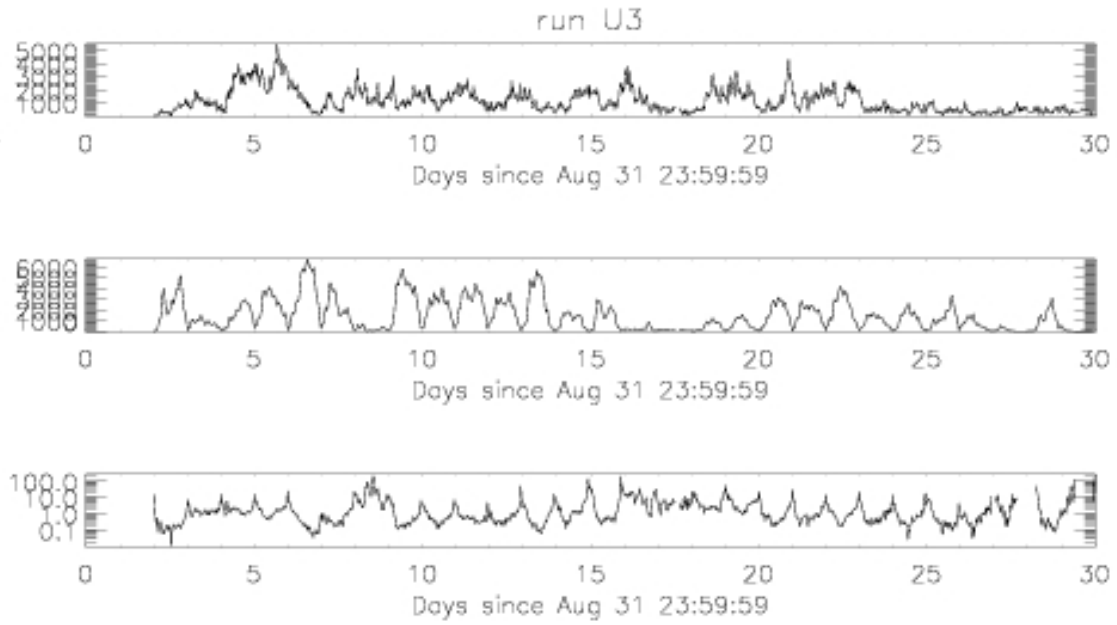

Figure 5.1: Comparing observed contrail numbers as a function of time through the month of September 2005, and a specific model scenario. In the upper panel we show the number of pixels per image frame classified as contrails. In the second panel we display the number of model contrail points, and in the third panel we show the ratio of the two.

5.1.2 Scoring method

For our first scoring strategy we chose to divide the region studied into a number of boxes (20x20), and simply tested whether the model predicted contrails in boxes that also contained observed contrails. We awarded 1 point to a box in which model and reality were in agreement and -1 for disagreements. By comparing the accumulated score for a map to how a random distribution of model contrails scored we can test the actual skill of the model. We shifted the model maps of contrails by random amounts in longitude and latitude, and used periodic boundary conditions, and thus retained most of the spatial correlation of a given scene, as well as the number of contrails. We calculated the skill in a scene as the fraction of the number of randomised scenes doing poorer than the real case. We tested 1000 randomisations for each half-hourly map. Each observed score thus becomes converted into a skill similar to a significance level, and these were accumulated for all scenes in a time interval and reported as an average over the scenes inspected. For different model runs we can then compare the skill in a relative sense and pronounce the winner. Repetitions of this scheme allows some testing of 'robustness' of the method in view of the stochastic nature of the Monte Carlo trials. We found that trials for the same model run typically was more robust than the differences between some model runs - i.e. the choice of contrail model parameters had a larger effect on the skill than the difference between two Monte Carlo trials of 1000 randomisations each for the same model.

5.1.3 Odds ratio

Stephenson (2000) has shown a method for investigating the relative quality of models based on odds ratios. This method was employed in Tompkins et al. (2007) to investigate the relative performance of two models that predicted contrails. We also implemented this method in order to compare to the stochastic method.

Table 5.1: 28-day runs. Column 1 gives the name of the model run Note that all runs, except CC9, have been performed with the nudging parameters in Figure 4.3, while CC9 was performed with 4.2. The columns give the values of the parameters in the model, which are: $RHi_{persist}$ is the limit allowed on relative humidity to form droplets, $w_{persist}$ is the limit on the vertical wind, D_h is a horizontal diffusivity, D_v is a vertical diffusivity, sig-v0 and sig-s0 are 'additional calibration parameters', and η is the fuel conversion efficiency. The five 'best' models under the three criteria for success have been labelled with an asterisk.

Model	$RHi_{persist}$	$w_{persist}$	D_h	D_v	sig-v0	sig-s0	w_0	η
CC1	0.85	-0.03	16.5	0.15	200	0	70	0.31
CC2	0.90	-0.03	16.5	0.15	200	0	70	0.31
CC3	0.95	-0.030	16.5	0.15	200	0	70	0.31
CC4	1.0	-0.030	16.5	0.15	200	0	70	0.31
CC5	0.8	-0.030	16.5	0.15	200	0	70	0.31
CC6	0.83	-0.030	16.5	0.15	200	0	70	0.31
CC7	0.87	-0.030	16.5	0.15	200	0	70	0.31
CC8	0.70	-0.030	16.5	0.15	200	0	70	0.31
CC9	0.87	-0.030	16.5	0.15	200	0	70	0.31
U1	0.7	-0.03	16.5	0.15	200	0	500	0.31
U2	0.7	-0.027	16.5	0.15	200	0	500	0.31
U3	0.7	-0.0333	16.5	0.15	200	0	500	0.31
U4	0.6	-0.03	16.5	0.15	200	0	500	0.31
U5	0.6	-0.027	16.5	0.15	200	0	500	0.31
U6	0.6	-0.033	16.5	0.15	200	0	500	0.31
U7	0.8	-0.03	16.5	0.15	200	0	500	0.31
U8	0.8	-0.027	16.5	0.15	200	0	500	0.31
U9	0.8	-0.033	16.5	0.15	200	0	500	0.31
Ww1	0.7	-0.030	16.5	0.15	200	0	70	0.31
Ww2	0.7	-0.027	16.5	0.15	200	0	70	0.31
Ww3	0.7	-0.033	16.5	0.15	200	0	70	0.31
Ww4	0.6	-0.03	16.5	0.15	200	0	70	0.31
Ww5	0.6	-0.027	16.5	0.15	200	0	70	0.31
Ww6	0.6	-0.033	16.5	0.15	200	0	70	0.31
Ww7	0.8	-0.03	16.5	0.15	200	0	70	0.31
Ww8	0.8	-0.027	16.5	0.15	200	0	70	0.31
Ww9	0.8	-0.033	16.5	0.15	200	0	70	0.31
yy1	0.9	-0.030	16.5	0.15	200	0	70	0.31
yy2	0.95	-0.030	16.5	0.15	200	0	70	0.31
z1	0.55	-0.03	16.5	0.15	200	0	70	0.31
z10	0.75	-0.027	16.5	0.15	200	0	70	0.31
z2	0.55	-0.024	16.5	0.15	200	0	70	0.31
z3	0.55	-0.036	16.5	0.15	200	0	70	0.31
z5	0.80	-0.060	16.5	0.15	200	0	70	0.31
z6	0.70	-0.020	16.5	0.15	200	0	70	0.31
z7	0.70	-0.040	16.5	0.15	200	0	70	0.31
z8	0.75	-0.030	16.5	0.15	200	0	70	0.31
z9	0.75	-0.033	16.5	0.15	200	0	70	0.31

6. Results

We have two basic sets of results. One set is based on the models in Table 5.1 which were run without outputting the information needed to calculate contrail optical depth off-line. The other set is based on the models in Table 6.4. We consider the first set in section 6.1 and then turn to the second set in section 6.2.

6.1 Model runs without contrail optical depth information

We summarise the results of the 28-day runs in Table 6.2 and in Figures 6.1 and 6.2. Despite a certain expected scatter in the SCORE, which has a stochastic nature due to the Monte Carlo trials employed, there does not seem to be a huge agreement between the two different methods of evaluating models against observations. As a compromise we select those models that appear to be doing well with both scoring methods, and these are CC5, CC6 and CC8. U1, U2, U3 and U7, WW1, WW3, WW7, WW8, and WW9, and Z7b and Z9. These models are characterised by parameter values in the ranges indicated in Table 6.1.

It is necessary to note here that the parameters varied here are the most influential. Other parameters (D_h, D_v,sig-v0 and η) could not be varied inside realistic limits and have particularly noticeable effects on the contrails, compared to variations in the three parameters listed in table 6.1: Those parameters were very influential on the production of contrails, with even small variations giving large changes in model contrails. It must also be noted that the parameters hardly have independent effects on the production of contrails - thus, a variation in one parameter can be compensated almost entirely by a variation in another parameter.

Table 6.1: List of best parameter values if contrail optical depths are **not** considered. These are the average best values given data from September 2005 over Germany. Especially $RHi_{persist}$ is important and is the easiest to constrain. The other two parameters have less influence on the comparison between observations and model predictions and are less well constrained.

Parameters	Range
$RHi_{persist}$	0.7 to 0.83
$w_{persist}$	-0.027 to -0.040
w_0	70 and 400

6.2 Considering the contrail optical depth

One limitation of the present study is that no consideration is made of whether the model contrails would actually be visible in reality - not in terms of width (which is taken into account) but in terms of the optical depth. It is known [Schumann, 1996] that contrails formed in warm surroundings will be optically thicker than contrails formed in cooler conditions, and a formal way to calculate the contrail optical depth, as a function of droplet size, air temperature, and vertical contrail thickness, is provided by Schumann. We have assumed the contrail optical depth model parameters listed in Table 6.3.

We calculated a special set of 10 model runs that allowed the off-line calculation of optical depth and consider these runs here. We select model contrails on the basis of their optical depths, and use limits of τ_{lim} from 0.0 and up to 0.3. Above 0.3 so few contrails are available that the analysis becomes

Table 6.2: 28-day runs compared. Column 1 gives the name of the model run - the parameters are listed in table 5.1. Column 2 gives the score as described in section 5.1.2. Column 3 gives the odds ratio, as described in section 5.1.3, while column 4 gives the correlation between the series for numbers of model and observed contrails.

Model	SCORE	ODDS/Z	R
CC3	0.339236	*1.44568	0.042768779
yy1	0.440554	1.27212	0.048776907
CC2	0.430157	1.26347	0.081460503
WW9	0.517675	1.33389	0.085397425
WW7	0.515658	1.33176	0.087959990
WW8	0.507727	1.33063	0.090865259
U7	0.520136	1.32562	0.091454563
U8	0.516433	1.31477	0.092325252
z9	0.529051	1.26482	0.10985167
Z3	0.502410	0.685317	0.11775380
U5	0.520972	0.846379	0.11973849
CC7	0.464160	1.28964	0.12209783
U6	0.524041	0.864425	0.13601485
WW6	0.521079	0.862026	0.13621914
WW3	*0.530192	1.16199	0.13858683
Z7b	*0.534582	1.14480	0.13895516
CC1	0.491109	*1.34243	0.13898131
WW4	0.521850	0.853632	0.13923358
U4	0.522143	0.860727	0.14045884
WW1	0.525145	1.15130	0.14149233
U3	*0.534742	1.15188	0.14264315
WW2	0.517346	1.14435	0.14552541
U1	0.528145	1.13682	0.14568821
U2	0.527703	1.13047	0.14913237
CC6.	0.512506	*1.38559	*0.15063719
Z6	0.506254	1.11310	*0.15462933
CC5	0.527284	*1.35889	*0.17050005
CC8	*0.535880	1.17630	*0.22146049

Table 6.3: List of parameter values assumed to calculate contrail optical depth according to the Schumann (1996) scheme.

Parameter	Value
a	3.448e-3
b	2.431
contrail thickness	200 m
r_{eff}	20 μ

meaningless. Figure 6.3 shows, for a point in time (September 7 2005 at 7AM) what the effect of various optical depth limits are on the match between observed contrails and those modelled.

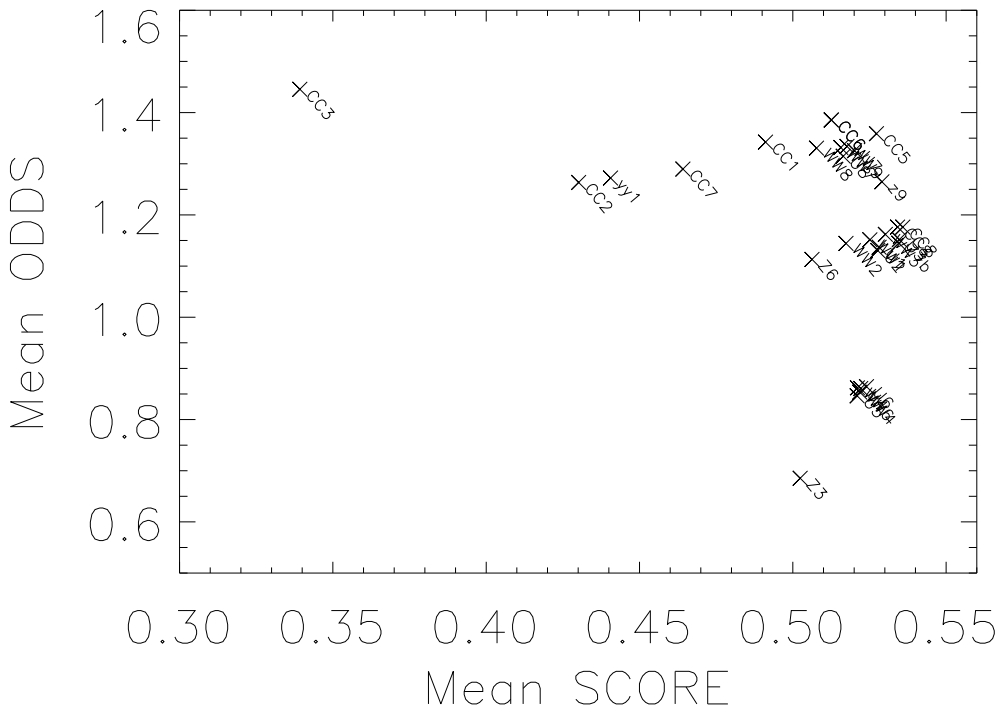

Figure 6.1: For 28-day runs, the mean SCORE is plotted against the mean odds-ratio (in units of standard deviations). Model names are plotted next to points, and refer to the names given in Table 6.2. Note that the SCORE is a stochastic estimate and therefore some scatter, or uncertainty, is present in the abscissa - the stochastic uncertainty is on the order of 0.002 SCORE units. The ordinate is the ratio of the natural logarithm of the odds-ratio and its parametric standard deviation.

In the Figure we see that the number of model contrails changes abruptly, on this day, for a limit on the optical depth somewhere between $\tau_{lim} = 0.075$ and 0.1. We also see the change in the number of contrails predicted in the eastern region of the box, which do not correspond to any detected contrails, as $\tau_{lim} = 0.075$ increases while at the same time the contrails in the upper left hand corner of the region do not disappear as readily. Qualitatively, this is encouraging as it points towards the possibility of limiting model parameters on the basis of the match between observations and model. Disappointingly though is that none of the detected contrails match any of the modelled ones closely - we mainly see a local match between contrail existence - not track-by-track.

Table 6.4 gives the parameter choices. Note that models AE4, AE8 and AE10 consist of a variation of $w_{persist}$ while other parameters are held constant, and that AE11, AE4 and AE13 constitute a variation in D_h with other things held constant. Model AE2 was an experiment to see whether there is sensitivity to a nudging parameter set which not only targets good performance for model winds with respect to the NCEP reanalysis, but also takes good performance in matching temperature into account.

Table 6.5 gives the SCORE, ODDS and correlations between observed contrails and modelled ones, for three settings of the optical thickness limit.

Inspection of Table 6.5 shows that the SCORE and the correlation values are strange - the SCORE is supposed to be the percentage of Monte Carlo trials that our model is better than, and it seems that very low values are possible. This corresponds to the model being *worse* than average random trails,

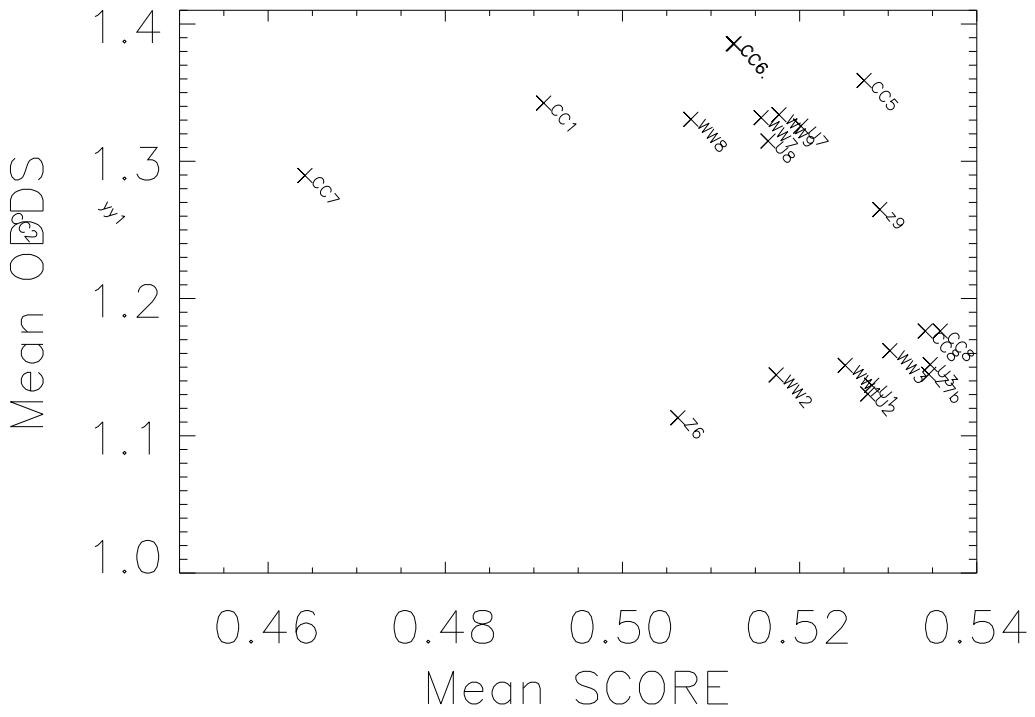

Figure 6.2: Detail of upper right-hand corner of Figure 6.1.

Table 6.4: Model parameter settings for model runs which allow the calculation of contrail optical depths.

Model	$RHi_{persist}$	$w_{persist}$	D_h	D_v	sig-v0	sig-s0	w_0	η	Notes
AE7	0.70	-0.030	16.5	0.15	200	0	70	0.31	NP: 4.2
AE3	0.75	-0.030	16.5	0.15	200	0	70	0.31	NP: 4.2
AE2	0.80	-0.030	16.5	0.15	200	0	70	0.31	NP: 4.4
AE1	0.80	-0.030	16.5	0.15	200	0	70	0.31	NP: 4.2
AE8	0.83	-0.025	16.5	0.15	200	0	70	0.31	NP: 4.2
AE11	0.83	-0.030	14.5	0.15	200	0	70	0.31	NP: 4.2
AE4	0.83	-0.030	16.5	0.15	200	0	70	0.31	NP: 4.2
AE13	0.83	-0.030	18.5	0.15	200	0	70	0.31	NP: 4.2
AE10	0.83	-0.035	16.5	0.15	200	0	70	0.31	NP: 4.2
AE5	0.85	-0.030	16.5	0.15	200	0	70	0.31	NP: 4.2
AE6	0.90	-0.030	16.5	0.15	200	0	70	0.31	NP: 4.2

which is something of an achievement. We also note that the correlations in the last column of Table 6.5 are small and unlikely to be significant - we have merely picked the most positive values. A discussion of why the SCORE method and the correlation does not appear to work well will not be attempted here, and we shall not use them further, restricting ourselves to the use of the ODDS method for model evaluation, as in [Tompkins, et al., 2007].

The ODDS column of Table 6.5 indicates that the models AE5 and AE6 are the best. These correspond to high values of $RHi_{persist}$(0.85 and 0.9). Considering the effect of a variation in D_h

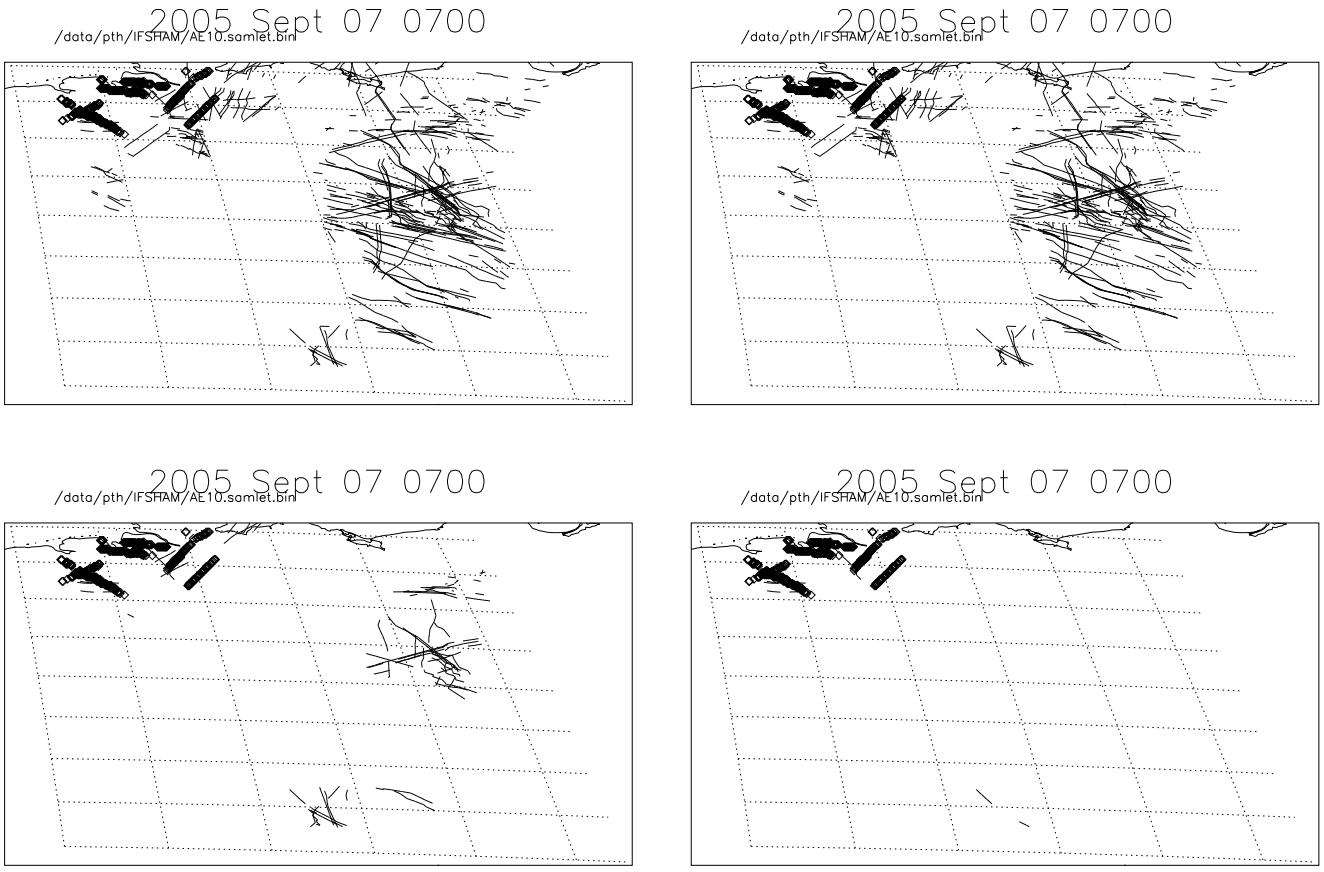

Figure 6.3: Effect of optical depth cutoff, on September 7 at 7AM, 2005. The upper left panel is for no cutoff, upper right is for $\tau_{lim} = 0.05$, lower left is for $\tau_{lim} = 0.075$ and the lower right is for $\tau_{lim} = 0.1$. The heavy symbols correspond to detected contrails, while the lighter lines correspond to model contrails.

(models AE4, AE11 and AE13) we note that the sensitivity in ODDS is very low. Considering the effect of a variation in $w_{persist}$ (models AE8, AE4 and AE10) we note that the sensitivity is low, but that there is a slight systematic dependence of ODDS on $w_{persist}$ with the least negative value ($w_{persist}$=-0.025) the winner.

The effect of using a modified set of nudging parameters (i.e. model AE2 vs. AE1) is almost nonexistent - as before, we conclude that the choice of nudging parameters is not very important - it is far more important to do nudging, of any realistic kind, than specifying a particular set of nudging parameters.

Table 6.5: Results from ten 28-day runs (sept 2 - 30), for three different cutoff limits on the contrail optical depth. In the three blocks below, the cutoff value is τ_{lim}=0.1, 0.2 and 0.3, respectively.

Run	SCORE	ODDS	R
AE1	0.477451	1.07477	0.1015
AE2	0.493367	1.07415	0.0731
AE3	0.514774	1.06450	0.1008
AE4	0.463380	1.09684	0.1171
AE5	0.448491	**1.10695**	**0.1336**
AE6	0.393098	1.05965	0.0517
AE7	**0.528235**	1.01206	0.0874
AE8	0.453878	1.09708	0.1250
AE10	0.469823	1.08868	0.1089
AE11	0.459135	1.09601	0.1155
AE13	0.463721	1.09536	0.1186
AE1	0.211454	1.26856	-0.0130
AE2	0.220098	1.28354	-0.0631
AE3	0.241299	1.12586	-0.0274
AE4	0.196636	1.33064	-0.0264
AE5	0.193749	1.38830	0.0260
AE6	0.173565	**1.43703**	**0.0804**
AE7	**0.267490**	1.03501	-0.0129
AE8	0.200842	1.34551	-0.0118
AE10	0.205718	1.32902	-0.0234
AE11	0.197821	1.32732	-0.0265
AE13	0.197885	1.33121	-0.0246
AE1	0.136341	1.52896	0.2180
AE2	0.133163	1.54790	0.3514
AE3	0.157027	1.48724	0.1402
AE4	0.143501	1.59536	0.2576
AE5	0.150378	**1.64611**	0.3619
AE6	0.145083	1.63272	**0.3756**
AE7	**0.165037**	1.47856	0.1327
AE8	0.141541	1.61177	0.2612
AE10	0.145403	1.58834	0.2578
AE11	0.141677	1.59650	0.2478
AE13	0.142371	1.59630	0.2575

7. Discussion

7.1 Is this a useful method for constraining contrail models?

We have seen that a comparison of observed contrails - detected in satellite images - and modelled contrails runs into certain practical problems.

First of all we have the issue of whether the detected contrails are a homogeneous sample at all times of the actual contrails - the question of whether the contrail-detection algorithm can be fooled by cloud boundaries, etc. An indication that something is wrong in the detection routine is the presence of contrails at midnight (see Figure 5.1 in observed data and the virtual absence in the models. In actual flight data, the number of flights drops sharply near midnight. This indicates that either our models simply do not generate enough long-lived contrails so that a substantial number survives to near midnight, or that a substantial fraction of the detected contrails are not real ones. This problem is present when individual contrails are not selected for analysis but area-means are considered.

Second, model parameters have turned out not to be independent in their effect on contrails. While a parameter controlling the sensitivity to spreading of contrails would be thought to be independent of a purely thermodynamic parameter describing the formation of contrails it all boils down to the same effect in practise - we can tune the number of model contrails in regions very effectively by use of several physically different parameters! The hunt for situations in which a thermodynamic parameter had a strikingly different effect on the distribution of contrails compared to the effect of a contrail-spreading parameter could not be found. It is not ruled out that such situations can be found in the large body of data we have, but so far none have been found.

Introduction of an additional cutoff to limit the model contrails inspected to those that have a chance of being seen from space has somewhat resolved our basic problem - for different realistic settings of the optical depth cutoff limit we find an indication that low values of $RHi_{persist}$ should be ruled out, and it was found that values in the $RHi_{persist}$=0.85 to 0.9 range gave better ODDS than lower values, and that there was some indication that a value of $w_{persist}$ of -0.025 was better than more negative values. Down-welling of contrails (i.e negative values of $w_{persist}$) causes their disappearance so a larger limit on $w_{persist}$ conserves contrail numbers. This may be an indication that the problem we saw when contrail optical depths were not considered has been broken - i.e. we now have contrail parameters that pull in different directions; they are not all trying to reduce the huge number of contrails formed in the model initially. This gives hope to the procedure of contrail model parameter estimation in the QUANTIFY project.

We find that the sensitivity to variations in model parameters other than $RHi_{persist}$ are quite small and we cannot usefully constrain all of them. Our main finding is therefore that values of $RHi_{persist}$ in the 0.85 to 0.9 range are indicated, along with a high lower limit on the allowable down-welling wind (i.e $w_{persist}$=-0.025 is better than $w_{persist}$=-0.035). Values larger than 0.9 for $RHi_{persist}$ cannot be ruled out, as we have not tested these, and a similar statement concerns the derived value of the limit on $w_{persist}$ (i.e. $w_{persist}$=-0.02 or -0.015 etc may prove better).

Selecting individual contrails for study could possibly help, if it were easy to find individual distinct contrails that easily match model contrails. This is not the case - we have been unable to match a single contrail in the observations convincingly to model contrails.

7.2 Model resolution

We have worked with a resolution of 1.125 by 1.125 degrees in the model - this introduces some coarseness in the physical conditions (winds and the thermodynamic properties) that invariably, despite interpolation, leads to mismatches between reality and model. Running the model with higher resolution might improve the comparability between model and observation.

7.3 Module transfer to EC-Earth?

At DMI the contrail module could be implemented in the EC-Earth model The current model version is based on IFS cycle31r1 and the standard atmospheric resolution is Tl159L62. Since the contrail model runs off-line using the atmospheric fields it should be rather simple to implement. However, there will be some work, adopting the nudging scheme. Further work including estimation of the impact on total cloud cover and radiative forcing could be done in the EC-Earth model environment.

8. References

[Déqué et al., 1994] Déqué, M., Dreveton, C., Braun, A., and Cariolle, D. (1994). The ARPEGE/IFS atmosphere model: a contribution to the French community climate modelling. *Max-Planck-Inst. Meteorol. Rep.*, page 349. Roeckner, E., Bäuml, G., Bonaventura, L., Brokopf, R., Esch, M., Giorgetta, M., Hagemann, S., Kirchner, I., Kornblueh, L., Manzini, E., Rhodin, A., and Schlese, U. (2003). The atmospheric general circulation model echam 5. Part i:Model description. *Max-Planck-Inst. Meteorol. Rep.*, page 349.

[Duda et al., 2004] Duda, D. P., Minnis, P., Nguyen, L., and Palikonda, R. (2004). A Case Study of the Development of Contrail Clusters over the Great Lakes. *Journal of Atmospheric Sciences*, 61:1132–1146.

[Guldberg and Nielsen, 2004] Guldberg, A. and Nielsen, J. K. (2004). Contrails and their impact on climate. *DMI scientific report 04-06*.

[Guldberg et al., 2005] Guldberg, A., Kaas, E., Déqué, M., Yang, S., and Vester Thorsen, S. (2005). Reduction of systematic errors by empirical model correction: impact on seasonal prediction skill. *Tellus Series A*, 57:575–+.

[Jeuken et al., 1996] Jeuken, A. B. M., Siegmund, P. C., Heijboer, L. C., Feichter, J., and Bengtsson, L. (1996). On the potential of assimilating meteorological analyses in a global climate model for the purpose of model validation. *Journal of Geophysical Research*, 101:16939–16950.

[Konopka, 1995] Konopka, P. (1995). Analytical Gaussian Solutions for Anisotropic Diffusion in a Linear Shear Flow. *J. Non-Equilib. Thermodyn.*, 20:78–91

[Mannstein, et al. 1999] Mannstein, H., Meyer, R., and P. Wendling (1999). Operational detection of contrails from NOAA-AVHRR-data. *Int. J. Remote Sensing*, vol 20, no 8, pp. 1641-1660.

[Ponater et al., 2002] Ponater, M., Marquart, S., and Sausen, R. (2002). Contrails in a comprehensive global climate model: Parameterization and radiative forcing results. *Journal of Geophysical Research (Atmospheres)*, 107:4164–+.

[Roeckner et al., 2003] Roeckner, E., Bäuml, G., Bonaventura, L., Brokopf, R., Esch, M., Giorgetta, M., Hagemann, S., Kirchner, I., Kornblueh, L., Manzini, E., Rhodin, A., and Schlese, U. (2003). The atmospheric general circulation model echam 5. Part i:Model description.

[Schumann, 1996] Schumann, U. (1996). On conditions for contrail formation from aircraft exhausts. *Meteorol. Zeitschrift*, 1:4–23.

[Schumann et al., 1995] Schumann, U., Konopka, P., Baumann, R., Busen, R., Gerz, T., Schlager, H., Schulte, P., and Volkert, H. (1995). Estimate of diffusion parameters of aircraft exhaust plumes near the tropopause from nitric oxide and turbulence measurements. *Journal of Geophysical Research*, 100:14147–14162.

[Stephenson, 2000] Stephenson, David B. (2000). Use of the "Odds Ratio" for Diagnosing Forecast Skill *Weather and Forecasting*, 15, issue 2, pp. 221-232.

[Sundqvist, 1978] Sundqvist, H. (1978). A parameterization scheme for non-convective condensation including prediction of cloud water content. *Quarterly Journal of the Royal Meteorological Society*, 104:677–690.

[Tompkins, et al., 2007] Tompkins, A. M.; Gierens, K.; Rädel, G. (2007) Ice supersaturation in the ECMWF integrated forecast system *Quarterly Journal of the Royal Meteorological Society*, vol. 133, issue 622, pp. 53-63.

[Yang, 2004] Yang, S. (2004). The DKCM Atmospheric Model. The Atmospheric Component of the Danish Climate Model. *Danish Climate Center Report 04-05*

8.1 Previous reports

Previous reports from the Danish Meteorological Institute can be found on:
http://www.dmi.dk/dmi/dmi-publikationer.htm